Materials Science and Technology (MS&T) 2013
October 27-31, 2013, Montreal, Quebec, Canada

Advanced Steel Metallurgy: Design, Processing, and Technological Exploitation

MICROSTRUCTURAL CHANGES OF A CONSTRUCTION STEEL CAUSED BY HOT DEFORMATION

José Ignacio Verdeja[1], María José Quintana[2], Roberto González[2], Luis Felipe Verdeja[1]
[1]E.T.S.I.M.O., Universidad de Oviedo, Independencia #13, Oviedo, 33004, Spain,
[2]Faculty of Engineering, Universidad Panamericana, Augusto Rodin #498, Mexico City, 03920, Mexico

Keywords: superplasticity, mechanical properties, fracture surface.

Abstract

A construction steel (shipbuilding strip) obtained by Advanced Thermomechanical Controlled Rolling Processes presents a room temperature banded ferrite-pearlite microstructure, and when superplastically deformed at 800°C with a strain rate of 5.85×10^{-5} s^{-1}, the bands disappear as there is grain boundary sliding and grain cluster rotation. Nevertheless, the superplastic deformation does not imply a decrease in mechanical properties, as room temperature tests with strain rates of 1.46×10^{-3} s^{-1} with the steel previously deformed in superplastic conditions (until a 110% of straining) result in similar mechanical data. If the steel is deformed at 750°C with low strain rates, cooling results in a microstructure formed only by ferrite and carbides (the pearlitic phase disappears). This behavior may be explained, from a thermodynamical point of view, by the effect of negative hydrostatic pressure during the tensile test and the pronounced ferrite- and carbide-former capacity of Ti and Nb microalloying elements.
The samples, tensile tested, in both the hot rolled raw state and superplastically deformed and then room temperature tested, show in the fracture surface SEM analysis almost identical features: decohesions surrounding MnS and (C,N)(Ti,Nb) precipitates and between ferrite and pearlite grains, as well as bedding.

Introduction

The manufacture and performance of steel parts for the automotive (and general) industry must take into account advanced themomechanical controlled rolling processes to obtain raw materials (in the form of strip or sheet) and subsequent deformations in either room or high temperature [1]. The microstructural analysis of these steels has to consider the industrial manufacture process and not only a laboratory scale evolution of grain size and phase formation [2,3]. If the strain hardening coefficient *n* (as measured by tension test with the ASTM standard) does not reach a minimum value of 0.1 in its hot rolling state, the material will present unstable plasticity upon yielding, severely restricting its potential uses [4], and therefore making cold-work operations such as bending, stretching and drawing unviable [5]. On the other hand, the mechanical resistance of steel parts deformed at high temperature, even when presenting superplastic behavior [6], must exhibit high enough values to allow their industrial use [7].
In order for a steel to present superplastic behavior the following is required [8]: a stable microstructure of fine equiaxied grains, an *m* coefficient (strain rate sensitivity exponent; $\sigma = K\dot{\varepsilon}^m$) values between 0.3 and 0.7, slow strain rates ($10^{-3} - 10^{-5}$ s^{-1}) and grain boundaries that allow grain sliding and rotation when stress is applied [9]. Furthermore, the steel must be deformed at a precise temperature, which is a fundamental characteristic in some superplastic

behavior models such as the one established by Ashby and Verrall [10]. This model proposes a theory (Grain Boundary Sliding, Diffusion-Accomodated Flow Rate Controlling) to describe superplasticity taking into account two mechanisms: the diffusion accommodated flow by grain boundary sliding and material transport by grain boundary diffusion [11], and the ordinary power-law creep (dislocation creep) which is a quasi-uniform flow mechanism that results in grain elongation.

The work presents mechanical tests and microstructural analysis of a steel sheet microalloyed with Ti and Nb, which after hot rolling is formed by bands (in the direction of rolling) of ferrite grains and pearlite zones [12-15]. Room temperature tensile tests data is compared to the tensile properties of samples deformed at high temperature (800°C) and then room temperature deformed, in order to evaluate the decrease in mechanical properties of the steel when deformed at the precise high temperature and strain rate to manufacture parts in a superplastic fashion [16]. Fracture surfaces of both types of samples were also compared to identify fracture mechanisms and the role of precipitates in the mechanical strength of the steel. On the other hand, samples deformed at 750°C were also evaluated, as at this temperature pearlite zones disappear, which is an indication of the displacement of the eutectoid point due to negative hydrostatic pressure during high temperature deformation, which must be taken into account during hot forming of the parts and industrial application of finished products [17].

Experimental procedure

The specified chemical composition for this steel (in weight %) according to the Euronorm UNE-EN 10025 is: C 0.168, Mn 1.361, Si 0.453, P 0.022, S 0.009, Cu 0.026, As 0.003, Al 0.028, Cr 0.035, Ti 0.026, V 0.002, Nb 0.033, Mo 0.004, Ni 0.031, Sn 0.002, Al (soluble) 0.027, B 0.0001, N 0.0055, Ca 0.0001 and H 2.00 ppm. In the same way, the specified mechanical properties are: higher yield stress (σ_y) = 447 MPa, rupture stress (σ_{max}) = 567 MPa, yield elongation with L_0 of 50 mm (El) = 31 % and impact resistance at -20 °C (KCV) = 96 J.

The samples for the tests were obtained from the steel sheet in an axis parallel to rolling direction and were machined in a cylindrical shape: 10 mm in diameter and calibrated gage length of either Lo = 57 or Lo = 30 mm (ASTM E21-05 standard).

High temperature tension tests were made at 750 and 800°C, as previous work had established superplastic behavior for this steel at these temperatures [13]. Different crosshead speeds were used, that combined with the two lengths of the samples resulted in different strain rates in order to obtain the hot deformation behavior (stress-strain rate curve) of the steel, and therefore locating the optimum superplastic conditions. An INSTRON 1195 model equipment for traction test with a load capacity of 100 kN was used along with an INSTRON 3112 model furnace which allows reaching temperatures as high as 1000°C. The tests were made without a protective atmosphere at crosshead speeds between 0.05 and 10 mm/min. Before the tests were performed, uniform heating from room to test temperature was made, lasting 1 hour, followed by a 5~10 min of stabilization. Variations of temperature inside the furnace were of maximum ±10°C.

Metallographic observations were carried out before and after the high temperature tests were made, analyzing the transverse sections of the samples in an axis parallel to the rolling direction. For most of the samples, normal grinding, polishing and etching with Nital-2 solution procedures were used. A Nikon Epiphot metallographic equipment was used to analyze different types of structural damages produced during superplastic deformation of selected samples. A scanning electron microscope (SEM) JEOL JSM-5600 with an electroprobe analyzer OXFORD model

6587 was used to observe characteristics such as decohesions, small precipitates and fracture surface. Thermo-calc software was used to simulate the effect of the negative hydrostatic pressure on the position of the eutectoid composition and temperature of a steel with these chemical characteristics.

Results

Figure 1 shows the curve of logarithm of yield stress/shear modulus vs. logarithm of strain rate for the steel tested, using data from Tables I and II (high temperature tests at 800°C). This curve has a sigmoidal shape, similar to the superplasticity model of Ashby-Verrall [10]. Deriving the third degree equation obtained from this curve, the m superplastic coefficient and the strain rate at which this coefficient would have the highest value for this steel can be found, in this case m reaches a value of 0.3 at a strain rate of $5.85 \times 10^{-5}\ s^{-1}$.

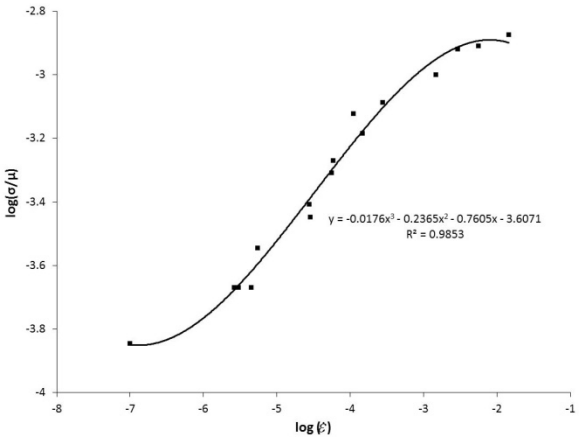

Figure 1. Logarithm of yield stress/shear modulus vs. logarithm of strain rate for the steel tested at 800°C.

Table I. Tension testing results obtained with different strain rates at 800°C.

Specimen initial length (mm)	Crosshead speed (mm/min)	Strain rate (s^{-1})	Yield stress (MPa)	Elongation (%)
30		$2.83x10^{-5}$	25 (creep)	Non-determined
30	0.05	$2.78x10^{-5}$	27.4	137.5
30	0.1	$5.56x10^{-5}$	34.4	181.7
57	0.2	$5.85x10^{-5}$	37.6	>110.0
30	0.2	$1.11x10^{-4}$	52.80	191.3
57	0.5	$1.46x10^{-4}$	45.8	>110.0
30	0.5	$2.78x10^{-4}$	57.3	92.7
57	5	$1.46x10^{-3}$	70	>110.0
57	10	$2.92x10^{-3}$	82.4	84.2
30	10	$5.56x10^{-3}$	86.2	105
23	20	$1.45\ x10^{-2}$	93.68	126.6

Table II. Creep tension testing results at 800°C.

Strain rate (s^{-1})	Applied stress (MPa)	Logarithm of strain rate	Logarithm of stress / shear modulus
$4.2x10^{-6}$	20	-5.38	-3.54
$4.5x10^{-6}$	15	-5.35	-3.67
$3.0x10^{-6}$	15	-5.52	-3.67
$2.6x10^{-6}$	15	-5.59	-3.67
$1.0x10^{-7}$	10	-7.00	-3.84

In order to evaluate the mechanical behavior of the steel after superplastically deformed at high temperature, room temperature tension tests were made on samples which had already suffered 110% of deformation at 800°C (5.85×10^{-5} s^{-1} of strain rate). Figure 2 shows the specimen in its original form (a), tension tested at room temperature (b), and its comparison with the sample superplastically deformed until 110% of elongation (c) and also tested at room temperature (d).

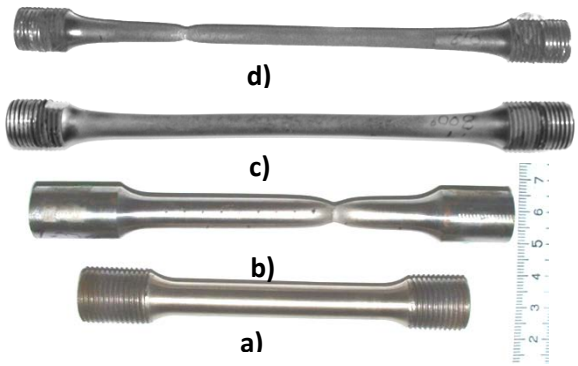

Figure 2. Tension test specimens of the steel samples in its hot rolled raw state (a), after tested at room temperature (b), after superplastically tested until a 110% of elongation at 800°C (c) and then room temperature tested (d).

Figure 3a shows the engineering stress-strain curves of both a specimen in its hot rolled raw state and one superplastically deformed until reaching 110% of deformation and then room temperature tension tested. It is evident that the superplastically deformed specimen presented lower yield stress (300 MPa) than the one in its hot rolled raw state (420 MPa), also it does not present higher and lower yield stress as the one shown in the specimen in its hot rolled raw state (it presents continuous yield elongation). The superplastically deformed specimen presents a lower uniform elongation but maintains a similar tension stress ~500 MPa, as well as a strain hardening coefficient n of 0.2 (necessary for manufacturing processes such as drawing of bending) [2]. Figure 3b compares the true stress-strain curves of both samples showing very similar strain hardening behavior and lower stress resistance (~50 MPa) for the high temperature deformed sample.

Figure 4 presents a comparison of the microstructure (metallographic observation) of samples with different conditions. The microstructure in both cases (in its hot rolled raw state and in the specimen superplastically deformed and then room temperature tension tested) is formed by ferrite and pearlite (previous austenite grains at temperatures above the eutectoid), however, the microstructure is more homogeneous and the grain size smaller in the superplastically deformed

specimen. Also, there is abundant precipitation in the superplastically deformed sample (Nb carbonitrides) induced by deformation.

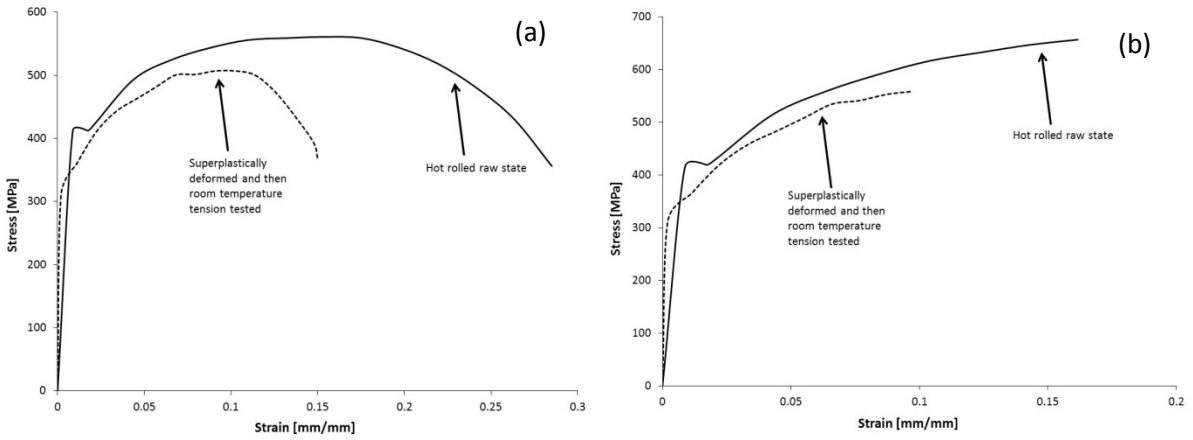

Figure 3. Stress vs. strain a) engineering curves b) true curves of a specimen in its hot rolled raw state and another one superplastically deformed and then room temperature tension tested.

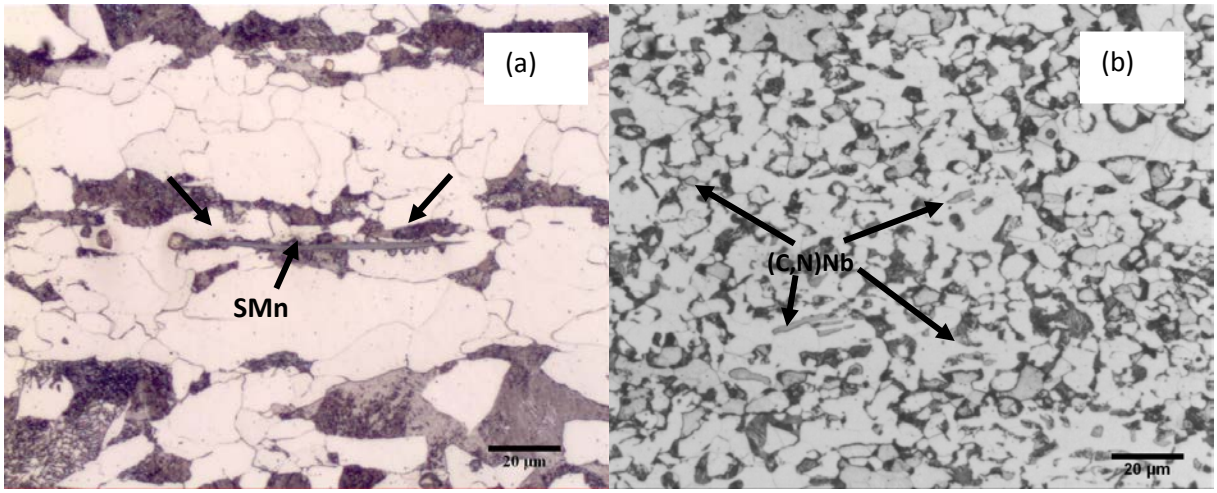

Figure 4. Micrographs of: a) steel in its hot rolled raw state, b) specimen superplastically deformed then room temperature tension tested

Figure 5 shows the SEM micrographs of the fracture surface of both the sample tested in its hot rolled raw state and the one present in the specimen superplastically deformed and then room temperature tension tested. In both cases decohesions are orientated with the main axis of the ellipse formed at the neck of the fracture sample. The superplastically deformed sample shows a smaller amount of decohesions though with larger size. Nevertheless, both fracture behaviors appear to be very similar.

High magnification SEM micrographs of the superplastically deformed fracture surface are shown in Figure 6, where the following may be noticed: large and small dimples (a), caused mainly by the decohesion of SMn and matrix (large ones) and possibly caused by the decohesion of (C,N)(Ti,Nb) and matrix (small ones).

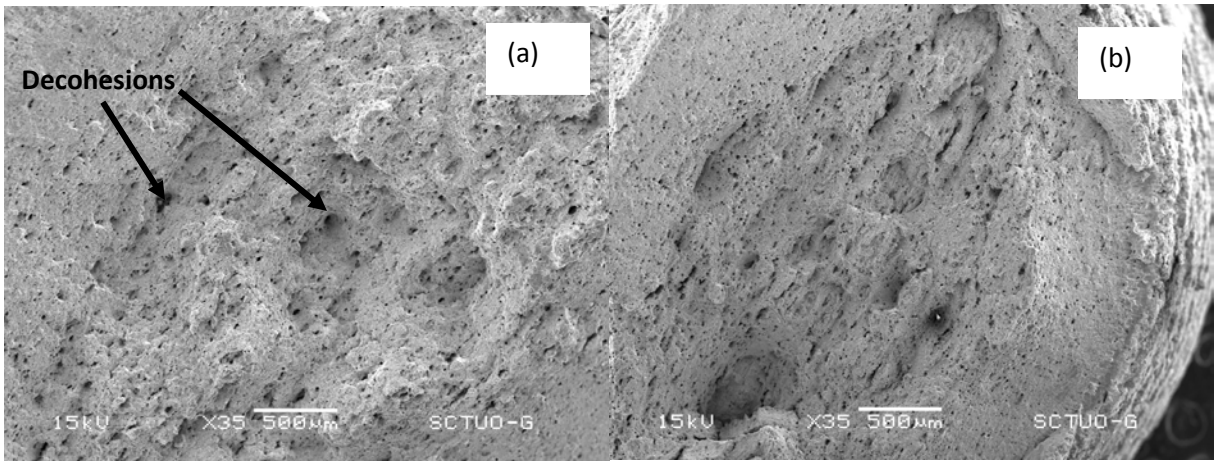

Figure 5. SEM fracture surface micrographs of samples tested in tension in the hot rolled raw state (a) and superplastically deformed and then room temperature tested (b).

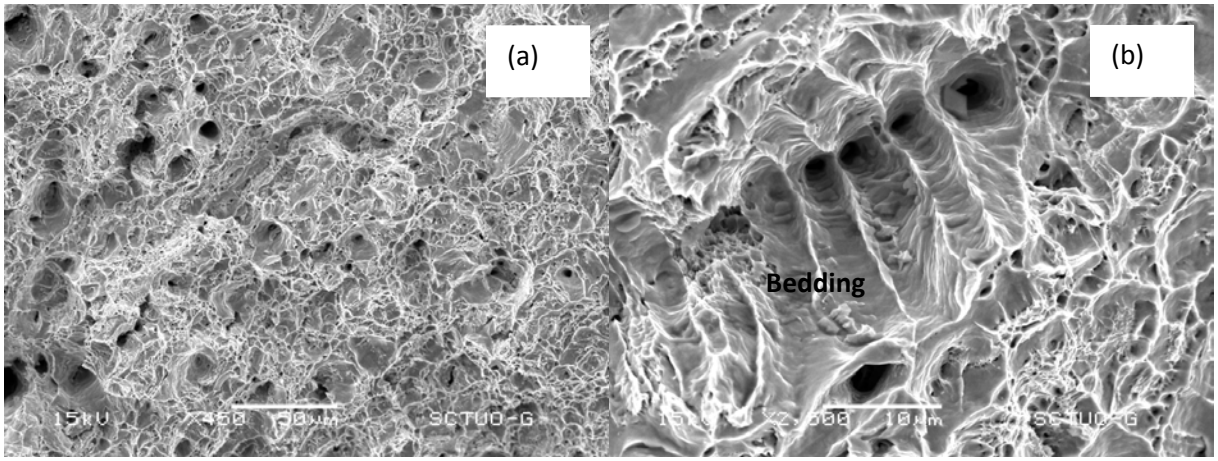

Figure 6. SEM micrographs of the fracture surface of a specimen superplastically deformed then room temperature tension tested

Discussion

The shape of the stress vs. strain rate curve (Figure 1) has the typical hot deformation behavior with the capacity to be deformed superplastically if values are in middle region of the curve. The microstructure of the steel at 800°C will be formed primarily by austenite grains which must present grain boundary sliding and rotation, in order to show superplasticity [14].

The curve shown in Figure 3a for the superplastically deformed and then room temperature tension tested is similar to those of interstitial free (IF) steels [4,18]. The growth of Nb and Ti carbonitrides precipitates during the high temperature test may explain this behavior, as they are no longer nanometric and absorb the free nitrogen present in the steel, resulting in a material without high and low yield stresses (continuous yield deformation). Another reason for this mechanical behavior can be the sweep out of N and C as interstitials elements absorbed by precipitates of Ti and Nb, leaving the ferritic matrix with an enhanced capacity to deform.

Figure 4b indicates that the high temperature deformation of the steel results in the disappearance of ferrite and pearlite bands, and the formation of small grains which resemble the microstructure of a dual-phase steel. This explains both the continuous yielding behavior and the high strength

of the material (almost as high as the original one) even though it was deformed at a very high temperature.
The decohesions along with the presence of MnS elongated inclusions may explain the low capacity of the superplastically deformed material to elongate, as maximum strain for this sample is close to 15%, while the hot rolled material reaches 30% at room temperature. Nevertheless, in the application of superplastically deformed parts, performance of the material is evaluated by its capacity to resist stress and not by its capacity to be deformed.
The difference in size of the decohesions observed on the fracture surface of the specimens (Figure 5) indicates that the superplastically deformed sample forms larger decohesions as these last ones were previously formed during the superplastic test at 800°C.
If the mechanisms of fracture of the superplastically deformed sample are considered, the presence of dimples and bedding (Figure 6) shows an enhanced capacity of the ferrite phase to deform while precipitates must suffer decohesion from the matrix in order to allow fracture. Figure 6b shows in its upper zone a precipitate with an almost squared geometric shape along with decohesions (dark zones) left by pearlite or precipitates when pulled out of the matrix.
If the microstructure of a sample deformed at 750°C is analyzed (Figure 7), the absence of pearlite can be explained through the following reasons: the transformation of austenite into ferrite and carbides is related to the strain induced precipitation; the specimen at this temperature suffered a negative hydrostatic pressure caused by straining which would move the eutectoid temperature towards higher temperatures (Figure 8) which would result in different zones of the phase diagram at 750°C and at 800°C. A negative pressure of 2000 bar would move the eutectoid point upwards by 25K. And from a temperature of 1000 to 1023K (750°C) the negative pressure required would be 1825 bar (~183 MPa), which is a pressure value similar in magnitude to the negative hydrostatic pressure created by intergranular and ductile decohesions as a result of the traction test. This behavior follows the Le Chatelier-Brown principle: if the $\gamma \rightarrow \alpha$ transformation is accompanied by volume increase ($\approx 1\%$), a negative pressure would move to the right the equilibrium of that reaction promoting the ferritic phase; and the Ti present in the steel (a ferrite-former element) would also move the eutectoid point.

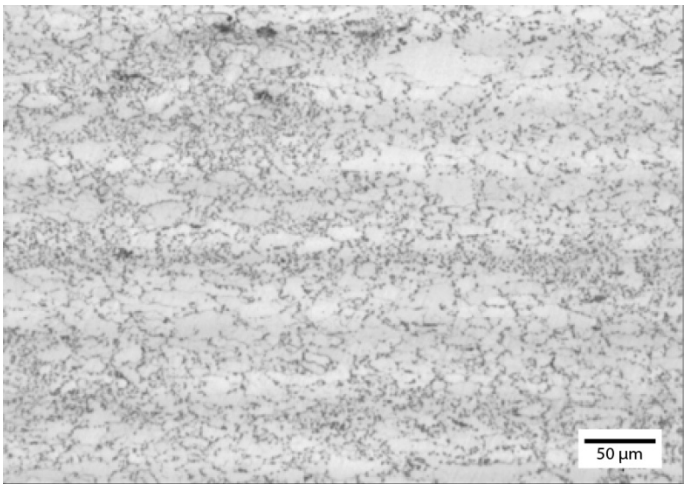

Figure 7. Micrograph of the steel after tension tested at 750°C

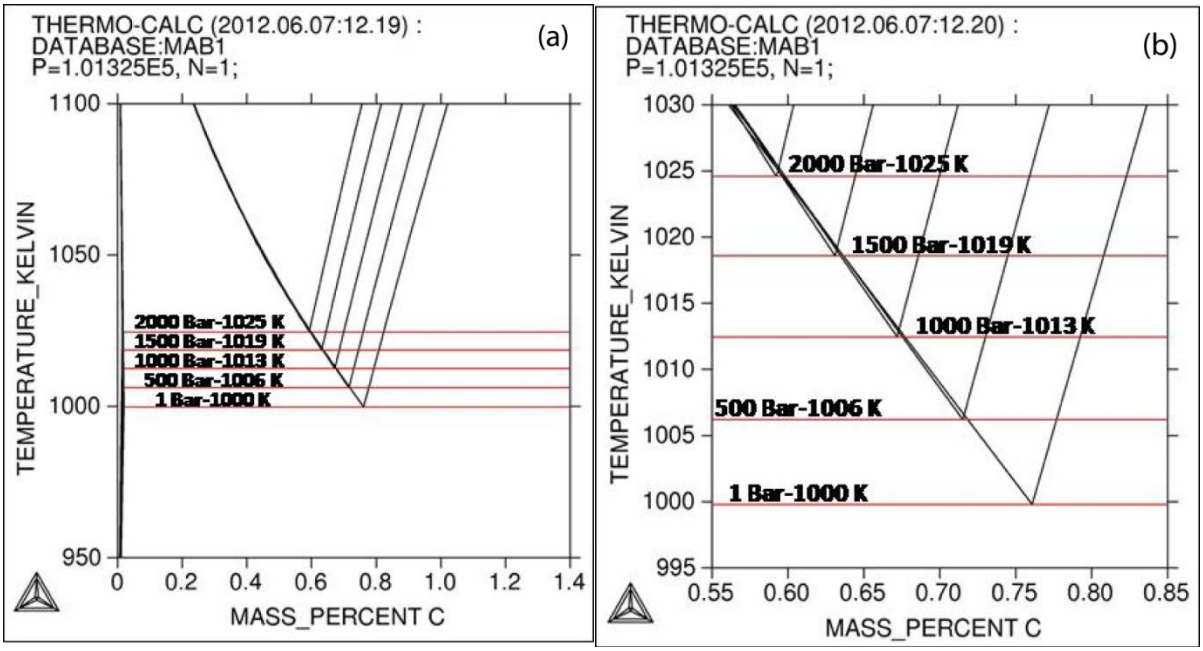

Figure 8. Change in the eutectoid composition and temperature as a result of changes in pressure.

Conclusions

The steel superplastically deformed, presents similar mechanical properties (especially its resistance) compared to the material in its hot rolled raw state. The HSLA steel (hot rolled raw state) becomes, after the superplastic deformation, an IF300 steel with ferritic-pearlitic microstructure, assuring that the steel superplastically deformed is a technologically viable material.

The Nb and Ti carbonitrides precipitates play an important role in the superplastic behavior of this steel, as shown in previous works, but also on the fracture surface profile of the steel, causing dimples, decohesions and bedding.

The negative hydrostatic pressure produced by tension testing of the steel at 750°C, combined with phase transformation-volumetric change results in a displacement of the eutectoid temperature and composition of the steel causing the disappearance of the pearlite bands and the formation of precipitates and small ferrite grains in its place. This phenomenon is also responsible for the formation of the 800°C microstructure.

References

1 A.A. Howe, “Ultrafine grained steels: industrial prospects”, *Journal of Materials Science and Technology*, 16 (2000), 1264-1266.

2 R. González, J.O. García, M.A. Barbés, M.J. Quintana, L.F. Verdeja and J.I. Verdeja, “Ultrafine Grained HSLA Steels for Cold Forming”, *Journal of Iron and Steel Research, International*, 17 (10) (2010), 50-56.

3 M. J. Quintana, R. Gonzalez, L. F. Verdeja and J. I. Verdeja, "Dual-Phase Ultrafine-Grained Steels Produced by Controlled Rolling Processes", *Materials Science and Technology (MS&T) 2011*, Columbus, Ohio, USA (2011), 504

4 R. Gonzalez, M.J. Quintana, L.F. Verdeja and J.I. Verdeja, “Ultrafine grained steels and the *n* coefficient of strain hardening”, *Memoria de Trabajos de Difusion Cientifica y Tecnica*, 9 (2011), 45-54.
5 W. A. Backofen, "Deformation processing", *Metallurgical Transactions*, 4 (1973), 2679-2699.
6 W.A. Backofen, I.R. Turner and H. Avery, “Superplasticity in an Al-Zn Alloy”, *Transactions of the ASM*, 57 (1964), 980-990.
7 G. Frommeyer and J. A. Jiménez, "Structural Superplasticity at Higher Strain Rates of Hypereutectoid Fe-5.5Al-1Sn-1Cr-1.3C Steel", *Metallurgical and Materials Transactions A*, 36A (2005), 295-300.
8 T.H. Alden, *Plastic deformation of materials. Review Topics in Superplasticity* (New York, NY: NY Academic Press, 1975), 225-266.
9 D.H. Avery and W.A. Backofen, *Transactions of the ASM*, 58 (1965), 551-562.
10 M. F. Ashby and R. A. Verrall, "Diffusion-accomodated flow and superplasticity", *Acta Metallurgica*, 21 (1973), 149.
11 J.A. Pero-Sanz, *Steels: Physical Metallurgy. Selection and Design* (Madrid, Spain: CIE–Dossat 2000, 2004) (in Spanish)
12 S. Fernandez, M.J. Quintana, J.O. García, L.F. Verdeja, R. González, J.I. Verdeja, “Superplasticity of ultrafine grained low-alloy steels”, *Memoria de Trabajos de Difusión Científica y Técnica*, 10 (2012), 45-56.
13 S. Fernández, M.J. Quintana, J.O. García, L.F. Verdeja, R. González, J.I. Verdeja, “Superplastic HSLA Steels: Microstructure and Failure”, *Journal of Failure Analysis and Prevention*, 13 (2013), 368-376.
14 F. A. Mohamed, "The role of boundaries during superplastic deformation", *Surface and Interface Analysis in Materials*, 31 (2001), 532-546.
15 T. Furuhara and T. Maki, “Grain boundary engineering for superplasticity in steels”, *Journal of Materials Science*, 40 (2005), 919-926.
16 J.I. Verdeja, M.J. Quintana, J.O. García, L.F. Verdeja, R. González, S. Fernandez, “Superplasticity of Ultrafine Grained Low-Carbon HSLA Steels”, *Materials Science and Technology (MS&T) 2012*, Pittsburgh, Pennsylvania, USA (2012), 945-956.
17 S. Vervynckt, K. Verbeken, B. López and J.J. Jonas, “Modern HSLA steel and role of non – recrystallisation temperature”, *International Materials Review*, 57 (2012), 187-207.
18 R. González, J.O. García, M.A. Barbés, M.J. Quintana, L.F. Verdeja, J.I. Verdeja, “Structural Ultrafine Grained Steels Obtained by Advanced Controlled Rolling”, *Journal of Iron and Steel Research, International*, 20 (1) (2013), 62-70.